Carbohydrate Polymers 101 (2014) 324–331

Contents lists available at ScienceDirect

Carbohydrate Polymers

journal homepage: www.elsevier.com/locate/carbpol

Synthesis, characterization and non-isothermal decomposition kinetic of a new galactochloralose based polymer

Gökhan Kök[a], Kadir Ay[b], Emriye Ay[b], Fatih Doğan[c], İsmet Kaya[d,*]

[a] Department of Chemistry, Faculty Sciences, Ege University, 35100 İzmir, Turkey
[b] Department of Chemistry, Faculty of Arts and Sciences, Celal Bayar University, 45140 Manisa, Turkey
[c] Secondary Science and Mathematics Education, Faculty of Education, Çanakkale Onsekiz Mart University, 17100 Çanakkale, Turkey
[d] Polymer Synthesis and Analysis Laboratory, Department of Chemistry, Faculty of Arts and Sciences, Çanakkale Onsekiz Mart University, 17020 Çanakkale, Turkey

ARTICLE INFO

Article history:
Received 27 July 2013
Received in revised form 28 August 2013
Accepted 18 September 2013
Available online 30 September 2013

Keywords:
Carbohydrate based polymer
Chloralose
Thermal analysis
Decomposition kinetic
Methacrylate

ABSTRACT

A glycopolymer, poly(3-*O*-methacroyl-5,6-*O*-isopropylidene-1,2-*O*-(*S*)-trichloroethylidene-α-D-galactofuranose) (PMIPTEG) was synthesized from the sugar-carrying methacrylate monomer, 3-*O*-methacroyl-5,6-*O*-isopropylidene-1,2-*O*-(*S*)-trichloroethylidene-α-D-galactofuranose (MIPTEG) via conventional free radical polymerization with AIBN in 1,4-dioxane. The structures of glycomonomer and their polymers were confirmed by UV–vis, FT-IR, ^{1}H NMR, ^{13}C NMR, GPC, TG/DTG–DTA, DSC, and SEM techniques. SEM images showed that PMIPTEG had a straight-chain length structure. On the other hand, the thermal decomposition kinetics of polymer were investigated by means of thermogravimetric analysis in dynamic nitrogen atmosphere at different heating rates. The apparent activation energies for thermal decomposition of the PMIPTEG were calculated using the Kissinger, Kim–Park, Tang, Flynn–Wall–Ozawa (FWO), Kissinger–Akahira–Sunose (KAS) and Friedman methods and were found to be 100.15, 104.40, 102.0, 102.2, 103.2 and 99.6 kJ/mol, respectively. The most likely process mechanism related to the thermal decomposition stage of PMIPTEG was determined to be a D_n deceleration type in terms of master plots results.

1. Introduction

In recent times, the basic raw materials used for polymers have expanded by including sugars such as glucose, galactose, fructose, and sucrose. Chemically connecting sugar moieties onto synthetic polymers is an individual method of functionalization of synthetic polymers. Through this method, the polymer is not only functionalized, but other desirable properties such as biodegradability can be achieved. This latter is a hotly debated and much researched topic nowadays (Varma, Kennedy, & Galgali, 2004). Sugar-carrying polymers, generally known as poly(vinylsaccharide)s, have been investigated intensively by researchers for a variety of applications, particularly in the biomedical field. Some potential applications for these types of polymers are drug delivery systems, dental medicine, bioimplants, contact lenses and tissue engineering (Pachence & Kohn, 1997, chap. 19). Furthermore, they have the advantage of being potentially biodegradable. Structurally, the poly(vinylsaccharide)s have a synthetic C—C backbone with pendant carbohydrate molecules. Since sugars are a good source of food for micro-organisms, many poly(vinylsaccharide)s have the potential to be utilized as biodegradable polymers. Syntheses of vinyl monomers prepared from isopropylidene and other protected sugars were comprehensively reviewed by Wulff, Schmid, and Venhoff (1996) and Varma et al. (2004) in their classical reviews. These sugar monomers are usually synthesized via the reaction of corresponding acid chloride (Carneiro, Fernandes, Figueiredo, Fortes, & Freitas, 2001) or anhydride (Lowe & Wang, 2007) with sugars in the presence of an organic amine such as pyridine. Sugar-carrying methacrylates such as 3-*O*-methacroyl-1,2:5,6-di-*O*-isopropylidene-α-D-glucofuranose (Kimura & Imoto, 1961), 6-*O*-methacroyl-1,2:3,4-di-*O*-isopropylidene-α-D-galactofuranose (Lowe & Wang, 2007), 1-*O*-acroyl-2,3:5,6-di-*O*-isopropylidene-α-D-mannofuranose (Salagean, Pascariu, Bandur, & Rusnac, 2009), monomethacroyl sucrose (Patil, Dordick, & Rethwisch, 1991) have already been reported. Homopolymerization or copolymerization of these sugar methacrylate monomers was performed via both atom transfer radical polymerization (ATRP) (Ohno, Tsujii, & Fukuda, 1998) and free radical methods such as a 2,2′-azobisisobutyronitrile (AIBN) (Carneiro et al., 2001). Poly(methacryoyl glucose) could be dyed by a water-soluble dyestuff (Varma et al., 2004). Owing to their low price, sugars such as sucrose and

* Corresponding author. Tel.: +90 286 218 00 18; fax: +90 286 218 05 33.
E-mail address: kayaismet@hotmail.com (İ. Kaya).

0144-8617/$ – see front matter © 2013 Elsevier Ltd. All rights reserved.
http://dx.doi.org/10.1016/j.carbpol.2013.09.065

D-galactose play an important role for this purpose. In this context, we decided to prepare a new isopropylidene protected vinyl saccharide, 3-*O*-methacroyl-5,6-*O*-isopropylidene-1,2-*O*-(*S*)-trichloroethylidene-α-D-galactofuranose. This compound was obtained from trichloroethylidene acetal of D-galactose, also known "galactochloralose" (Anıl, Yüceer, & Yüceer, 1983). Monosaccharides mostly react in their furanose forms with chloral to give trichloroethylidene acetals. Thus, 1,2-*O*-trichloroethylidene acetals of D-glucofuranose (Forsen, Lindberg, & Silvander, 1965), D-galactofuranose (Anıl et al., 1983), D-arabinofuranose (Salman, Makinabakan, & Yüceer, 1994) and D-mannofuranose (Salman, Kök, & Yüceer, 2004) are known. 1,2-*O*-(*R*)-Trichloroethylidene-α-D-glucofuranose is a commercially available compound, also known as α-chloralose, which is used as an anesthetic for animals (Metz, Ise, & Haberle, 1996). Additionally, trichloroethylidene acetals are suitable protecting groups for the synthesis of some biologically important compounds (Kök & Salman, 2012) and antimicrobial chloralose derivatives are also known (Yenil, Ay, Ay, Oskay, & Maddaluno, 2010). On the other hand, thermogravimetric analyses of polymer samples have been extensively utilized for determining decomposition characteristics and also for determining kinetic parameters. However, non-isothermal thermogravimetry has been widely used to investigate the thermal stability characteristic of various substances, including the polymer pyrolyzes. Several papers have shown that nonisothermal thermogravimetric analysis is a powerful tool to characterize the thermal decomposition of polymers (Doğan, Akat, Balcan, Kaya, & Yürekli, 2008; Doğan, Şirin, Kaya, & Balcan, 2010; Şirin, Doğan, Balcan, & Kaya, 2009). Doğan, Kaya, and Bilici (2011) investigated the thermal behavior, kinetic and thermodynamic parameters of many polyphenol-based polymeric materials using different thermogravimetric methods. They reported for first time that the thermal decomposition processes of so-called polymeric materials follow a diffusion model (Dilek, Doğan, Bilici, & Kaya, 2011; Kaya, Doğan, & Bilici, 2009). Budrugeac and Segal (2008) studied the decomposition mechanism and kinetic parameters of an epoxy system using isoconversional and multivariate non-linear regression methods. Briefly, the thermal decomposition kinetics for many polymer species has been studied in the literature. However, the thermal decomposition kinetics and process mechanisms of a carbohydrate-based polymer are presented for the first time in this study. Accordingly, a new sugar derivative of the methacrylate polymer was synthesized from 3-*O*-methacroyl-5,6-*O*-isopropylidene-1,2-*O*-(*S*)-trichloroethylidene-α-D-galactofuranose by free radical polymerization with AIBN in 1,4-dioxane. The structures of the resulting compounds were confirmed by UV–vis, FT-IR, ^{1}H NMR and ^{13}C NMR. Further characterization processes were performed by thermogravimetry–differential thermal analysis (TG–DTA), gel permeation chromatography (GPC), scanning electron microscope (SEM) and solubility testing. Also, the kinetics of the thermal decomposition of a carbohydrate-based sugar polymer was investigated with the TG technique. The kinetic parameters related to the decomposition kinetics of a carbohydrate-based sugar polymer were calculated using the Kissinger (Kissinger, 1957), Kim–Park (Kim & Park, 1995), Tang (Tang, Liu, Yang, & Wang, 2004), Flynn–Wall–Ozawa (Flynn & Wall, 1966; Ozawa, 1965) (FWO), Kissinger–Akahira–Sunose (Akahira & Sunose, 1971) (KAS) and Friedman (Friedman, 1965) (FR) methods under an N_2 dynamic atmosphere and at different heating rates of 5, 10, 15 and 20 °C/min. The mechanism function and pre-exponential factor were determined by master plots curves.

2. Experimental

TLC and column chromatography were performed on pre-coated aluminum plates (Merck 5554) and silica gel G-60 (Merck 7734), respectively. Methacrylic anhydride and all the solvents were commercially obtained as chemical pure reagents and used without further purification.

2.1. Synthesis of MIPTEG

5.0 mL of methacrylic anhydride was added to a solution of 5,6-*O*-isopropylidene-1,2-*O*-(*S*)-trichloroethylidene-α-D-galactofuranose (5.0 g, 14.3 mmol) (Anıl et al., 1983) in 30 mL of dry pyridine. The mixture was stirred at room temperature and after 24 h. TLC (Toluen:MeOH, 8:2) showed that no original starting compound remained. The solvent was evaporated under reduced pressure at 35 °C and the residue was extracted with CH_2Cl_2 (3 mL × 50 mL). The combined extracts were dried with anhydrous sodium sulfate and evaporated under reduced pressure. The syrupy residue was purified using column chromatography on silica gel eluted with CH_2Cl_2:MeOH (50:1) and 5.44 g of a monomeric syrupy compound were obtained, yield: 91%. The resulting monomer was characterized using spectroscopic analyses such as UV–vis, FT-IR, ^{1}H NMR and ^{13}C NMR techniques. The synthetic strategy is outlined in Scheme 1.

UV–vis (λ_{max}) (DMSO): 278 nm, FTIR (ATR): 2982–2897 ν (C—H), 1711 ν (C=O), 1610 ν (C=C), 1153 ν (COC), 798 cm^{-1} ν (CH—Cl). ^{1}H NMR ($CDCl_3$): δ 6.34 (d, 1H, $J_{1,2}$ = 4.4 Hz, H-1), 6.15 (bs, 1H, CH_2=C—CH_3), 5.74 (s, 1H, $CHCCl_3$), 5.67 (dt, 1H, CH_2=C—CH_3, J_{CH_2} = 1.6 Hz, J_{CH_2,CH_3} = 1.6 Hz), 5.16 (d, 1H, $J_{3,4}$ = 1.6 Hz, $J_{2,3}$ = 0.0 Hz, H-3), 5.09 (d, 1H, H-2), 4,35 (dd, 1H, H-5), 4.14 (m, 1H, H-4), 4.09 (dd, 1H, $J_{6a,6b}$ = 8.4 Hz, $J_{5,6a}$ = 6.8 Hz, H-6a), 3.96 (dd, 1H, $J_{5,6b}$ = 7.2 Hz, H-6b), 1.96 (bs, 3H, CH_2=C—CH_3), 1.49 and 1.42 (s, 6H, $(CH_3)_2$C). ^{13}C NMR ($CDCl_3$): δ 166.4 (C=O), 135.4 (CH_2=C—CH_3), 127.6 (CH_2=C—CH_3), 110.6 and 109.8 ($CHCCl_3$ and C-1), 107.8 ($(CH_3)_2$C), 99.5 ($CHCCl_3$), 87.4, 87.0, 78.6, 75.8, 72.4 (C-2, C-3, C-4, C-5, C-6), 26.6 and 25.7 ($(CH_3)_2$C), 18.3 (CH_2=C—CH_3). Anal. Calcd. for MIPTEG: C, 57.50; H, 6.70. Found: C, 58.07; H, 6.12.

2.2. Synthesis of PMIPTEG

PMIPTEG was obtained through a conventional free radical polymerization using 2,2′-azobisisobutyronitrile (AIBN) (2%, based on the total weight of the monomer) as initiator in 5 mL of 1,4-dioxane

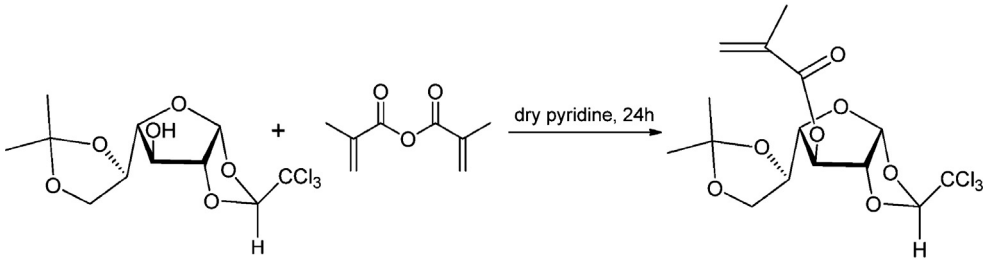

Scheme 1. Synthetic method for the preparation of MIPTEG.

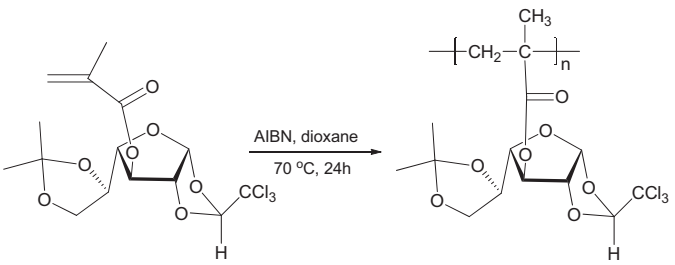

Scheme 2. Synthetic route for PMIPTEG.

at 70 °C for 24 h with 92% conversion in an all glass Schlenk flask. The resulting polymer was precipitated in ethanol and dried under vacuum at 40 °C for 24 h and characterized using various spectroscopic methods (yield: 95%). The synthetic route is presented in Scheme 2.

UV–vis (λ_{max}) (DMSO): 253, 375 nm, FTIR (ATR): 2986 ν (C—H), 1730 ν (C=O), 1153 ν (COC), 809 cm^{-1} ν (CH—Cl); ^{1}H NMR (DMSO-*d6*): δ 6.43 (H-1), 5.52 (CH—CCl_3), 4.82 (H-3), 4.52 (H-2), 4.01 (H-5), 3.81 (H-4 and H-6a), 3.67 (H-6b), 1.28–0.60 (H-8, H-9, H-10 and H-11); ^{13}C NMR (DMSO-*d6*): δ 179.7 (C=O), 111.7 ($CHCCl_3$), 109.2 (C-1), 107.0 (C-9), 99.3 ($CHCCl_3$), 86.2, 78.8, 74.1, 65.3 (C-2, C-3, C-4, C-5 and C-6), 47.8, 30.4, 26.4, 20.1, 19.3 (C-10, C-11, C-13, C-14 and C15). Calcd. for PMIPTEG: C, 57.26; H, 7.00. Found: C, 57.97; H, 7.32.

2.3. Characterization techniques

Ultraviolet–visible (UV–vis) spectra were measured with the Perkin-Elmer Lambda 25. The spectral analyses of MIPTEG and PMIPTEG were recorded using a Mattson FT-IR-1000 spectrometer with KBr discs (4000–400 cm^{-1}). ^{1}H (400 MHz) and ^{13}C NMR (100 MHz) spectra of PMIPTEG were recorded on a Varian AS 400 instrument, and NMR spectra of MIPTEG were recorded on the Varian XL200. TMS was used as an internal standard. Elemental analysis was carried out with a Carlo Erba 1106. The number-average molecular weight (M_n), weight-average molecular weight (M_w) and polydispersity index (PDI) of PMIPTEG were determined by using a Huwlett Packard GPC–SEC system calibrated with polystyrene standards at 30 °C using THF as an eluent at a flow rate of 1.0 mL/min. The TG/DTA and DSC curves were obtained using a Shimadzu TGA-50 thermobalance and a Shimadzu differential scanning calorimeter (DSC) DSC-50 model, respectively. The TG measurements were performed by using a dynamic nitrogen furnace atmosphere at a flow rate of 60 mL/min up to 1273 K. The heating rates were 5, 10, 15 and 20 K/min and sample sizes ranged in mass from 8 mg to 10 mg. Platinum was used for the sample container. DSC experiments were performed using aluminum pans with 5 mg samples in the temperature range of 20–450 °C at a heating rate of 10 K/min. All experiments were performed twice for repeatability, and the results showed good reproducibility with small variations in the kinetic parameters. α-Al_2O_3 was used as a reference material. The surface morphology of PMIPTEG was evaluated via scanning electron microscopy (SEM), using a Philips XL 30S FEG apparatus.

3. Results and discussion

3.1. Characterization studies

As shown in Scheme 1, 5,6-*O*-isopropylidene-1,2-*O*-(*S*)-trichloroethylidene-α-D-galactofuranose reacted with methacrylic anhydride in pyridine at room temperature to give 3-*O*-methacroyl-5,6-*O*-isopropylidene-1,2-*O*-(*S*)-trichloroethylidene-α-D-galactofuranose (MIPTEG). Then PMIPTEG was obtained

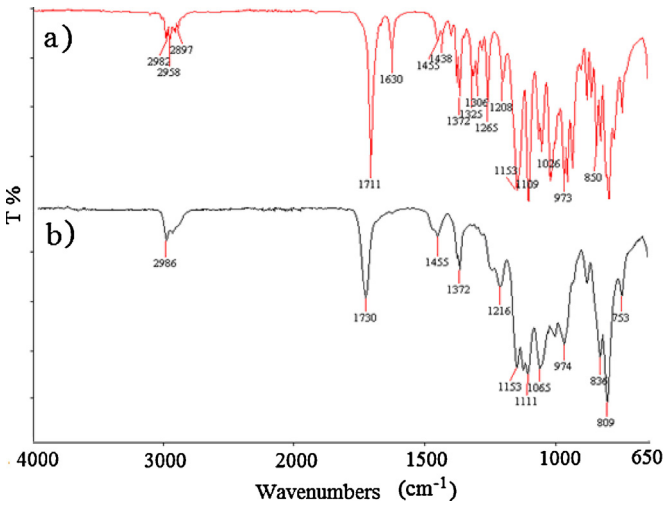

Fig. 1. FT-IR spectra of (a) MIPTEG and (b) PMIPTEG.

through the homopolymerization of MIPTEG with 2,2′-azobisisobutyronitrile (AIBN) as a radicalic initiator in a 1,4-dioxane solution at 70 °C. PMIPTEG was isolated as a white powder in high yield (95%). MIPTEG and PMIPTEG were structurally characterized by using different spectral techniques: FT-IR, ^{1}H and ^{13}C NMR. Further characterization of PMIPTEG was carried out by GPC, SEM, TG/DTG–DTA and DSC analyses. PMIPTEG was soluble in common organic solvents, such as dimethylsulfoxide (DMSO), dimethylformamide (DMF), dimethylacetamide (DMA), *N*-methyl-2-pyrrolidone (NMP). However, it was insoluble in chloroform, dichloromethane, hexane, toluene, and methanol. Infrared spectroscopy is widely used for analysis of poly(vinyl saccharide)s. In almost all cases, the disappearance of C=C bond is a means for deciding the completion of polymerization of the vinyl sugars.

Representative FT-IR spectra of MIPTEG and PMIPTEG are provided in Fig. 1. In the FT-IR spectrum of the glycomonomer and glycopolymer, the bands observed at approximately 1711 and 1730 cm^{-1} for both MIPTEG and PMIPTEG, respectively, are due to the characteristic carbonyl vibrations of the methacrylate groups. The intensity of the vinyl linkage observed at 1630 cm^{-1} for PMIPTEG drastically decreased and shifted to a longer wave number after polymerization, which was attributed to the absence of conjugation between C=O and C=CH_2 linkages. On the other hand, the extended spectrum of polymers compared to monomers is also common for sugar-based polymers bearing vinyl groups and suggests the presence of the polymerized structure of MIPTEG with broad chain dispersity. The band at 1630 cm^{-1} which is the most important and characteristic absorption for vinyl structure is also observed for monomer. However in the case of polymers, this band disappeared.

The ^{1}H NMR peak performance of the glycomonomer (MIPTEG) is presented in Fig. 2, and shows the specific double bond protons at 5.67–6.15 ppm (H-10) and the methyl group at 1.96 ppm (H-11) from the methacroyl moiety. The protons of the sugar moiety of MIPTEG were observed at 6.34 (H-1), 5.74 (H-7), 5.16 (H-3), 5.09 (H-2), 4.35 (H-5), 4.14 (H-4), 4.09 and 3.96 (H-6), 1.49 and 1.42 ppm (H-8 and H-9) in the spectrum (in Fig. 2a). However, disappearance of characteristic vinyl peaks (H-10) for the methacroyl moiety of the monomer can be observed in the ^{1}H NMR spectrum of PMIPTEG (Fig. 2b).

Also, the ^{13}C NMR peak performance of MIPTEG and PMIPTEG were described in Fig. 3 and similarly, the expected indications were observed. In the ^{13}C NMR spectrum of MIPTEG (Fig. 3a), the

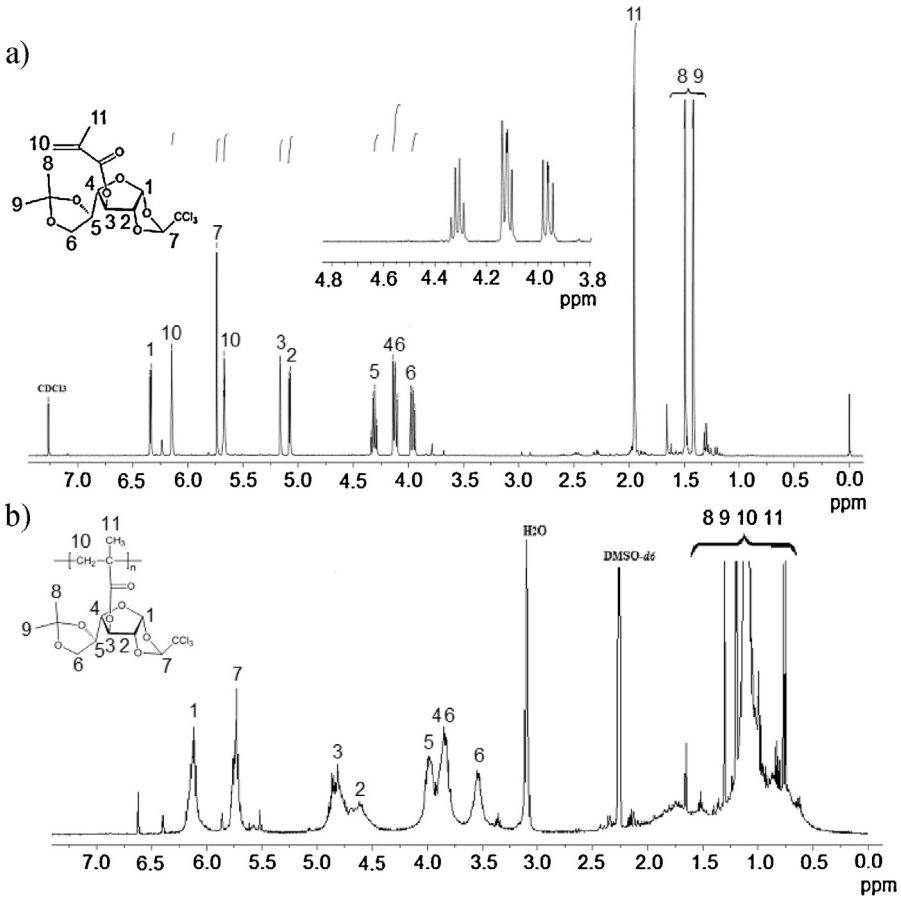

Fig. 2. ^{1}H NMR spectra of (a) MIPTEG and (b) PMIPTEG.

peaks at 127.7 and 135.4 ppm (C-13 and C-14) were assigned the vinyl carbon and a carbonyl peak was observed at 166.4 ppm. In the case of the polymer, it was observed that vinyl protons disappeared after the polymerization process and alkyl group peaks (C-13, C-14) of glycopolymer appeared in the range from 47.6 to 22.1 ppm. Also, vinyl carbons of PMIPTEG shifted to a higher field as a result of increased electron intensity. ^{13}C NMR peaks of the sugar moiety for both the polymer and the monomer were observed as predicted from C-1 to C-11 in Fig. 3.

The uncleavage of the isopropylidene groups MIPTEG and PMIPTEG are understood from NMR spectra. IR and NMR analyses clearly indicated that MIPTEG was successfully obtained and that PMIPTEG was polymerized by free radical reaction. The number average molecular weight (M_n), mass average molecular weight (M_w) and polydispersity index (PDI) of PMIPTEG were found to be 9300 g/mol, 13,400 g/mol and 1.44, respectively. The thermal properties of MIPTEG and PMIPTEG were studied using the TG/DTG and DTA techniques from ambient temperature to 1000 °C under nitrogen atmosphere. Typical TG/DTG and DTA curves for MIPTEG and PMIPTEG in N_2 were presented in Fig. 4. The initial and final temperatures and total mass losses in the thermal decomposition of compounds were determined, together with temperatures of the highest rate of decomposition (DTG_{max}).

MIPTEG and PMIPTEG exhibited the stage one decomposition process. From the TG curve for MIPTEG, it appeared that the sample decomposed with a mass loss of 96.3% in the temperature range 199–435 °C. However, endothermic thermal effects at 121 and 311 °C in the DTA profile correspond to the solvent peak (absorbed in syrup) and thermal decomposition of MIPTEG, respectively. PMIPTEG is thermally stable up to 218 °C and decomposed in the temperature range from 218 °C to 581 °C with a 92.30% weight loss. The temperature related to the maximum decomposition rate for MIPTEG was determined to be 288 °C in the DTG curve. This temperature for PMIPTEG is 303 °C. As expected, these results showed that PMIPTEG is more stable than MIPTEG. The differential scanning calorimetry (DSC) was used to investigate the thermal properties of PMIPTEG. The DSC curve of PMIPTEG exhibited an endothermic peak at 74 °C and an exothermic peak at 317 °C. These peaks in the DSC curve were attributed to the glass transition temperature and the thermal decomposition of PMIPTEG, respectively. The morphological properties of the resulting polymer were investigated by means of SEM analysis. SEM photographs of powdered PMIPTEG are given in Fig. 5. The sequence bead structures on the main chain in Fig. 5 were observed for the powdered PMIPTEG samples. In addition, as shown in the SEM image of the selected area, PMIPTEG had a linear backbone structure. Also, the linear polymer chains were very condensed, unhomogeneous and did not exhibit a well-ordered structure or shape. They consisted of long and thin channels. The average particle diameter of randomly oriented ellipsoids is lower than approximately 1 μm.

On the other hand, isoconversional methods such as FWO, Tang, KAS, FR, Kim–Park and Kissinger were used to investigate the kinetic parameters (activation energy, *E*, frequency factor, *A*) related to the solid state thermal decomposition of PMIPTEG. Kinetic analysis of PMIPTEG was investigated using the thermogravimetry technique with samples of 8–10 mg at heating rates of 5, 10, 15 and 20 °C/min under a nitrogen atmosphere (60 mL/min). A typical dynamic TG/DTG–DTA curve for PMIPTEG at a heating rate of 10 °C/min in N_2 is represented in Fig. 4b. Additionally, the solid state degradation mechanism of PMIPTEG was determined by

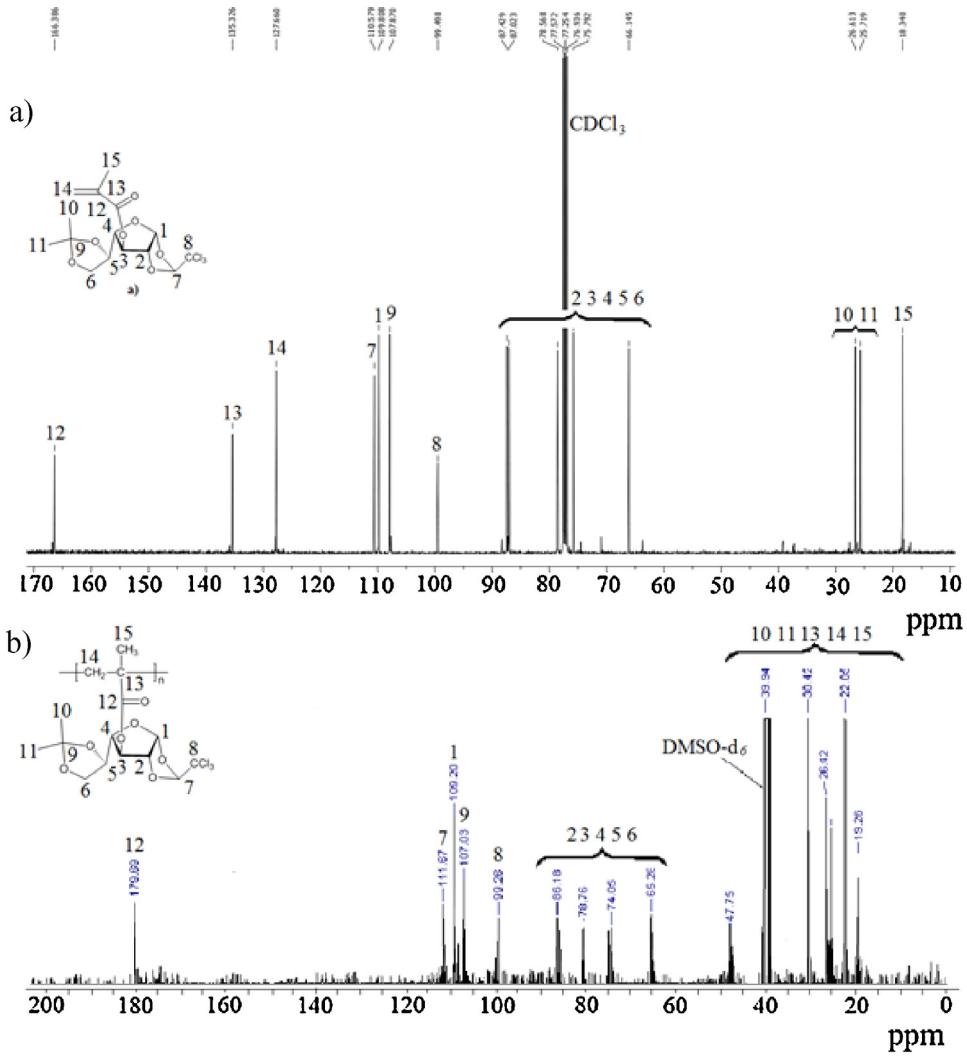

Fig. 3. ^{13}C NMR spectra of (a) MIPTEG and (b) PMIPTEG.

master plots of TG/DTG curves under N_2. All of the TG/DTG–DTA curves which were obtained at several heating rates for PMIPTEG showed that the thermal decomposition took place mainly in one stage. However, TG-curves are characteristically very similar to each other. In this work, the Kissinger and Kim–Park procedures are the primary thermogravimetric methods. TG data of PMIPTEG were initially analyzed with the Kissinger procedures as it is independent of the heating rate and any thermal decomposition mechanisms. This method uses the maximum decomposition temperature (T_{max}) at which the rate of mass loss is the highest. This method may briefly be expressed by the following equation.

$$\ln\left(\frac{\beta}{T_{max}^2}\right) = \left\{\ln\frac{AR}{Ea} + \ln[n(1-\alpha_{max})^{n-1}]\right\} - \frac{Ea}{RT_{max}} \quad (1)$$

The activation energy can be calculated using Eq. (1) without knowing the solid state degradation reaction mechanism. The slope of the line drawn between ln (β/T_{max}^2) versus $1000/T_{max}$ gives

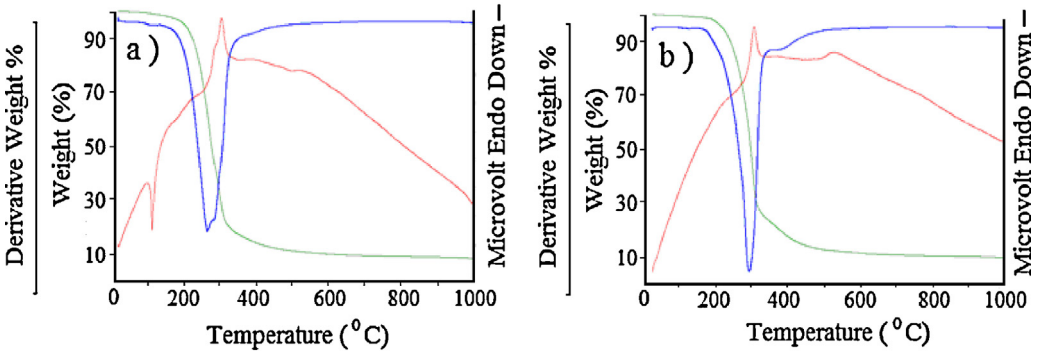

Fig. 4. TG curves of (a) MIPTEG and (b) PMIPTEG.

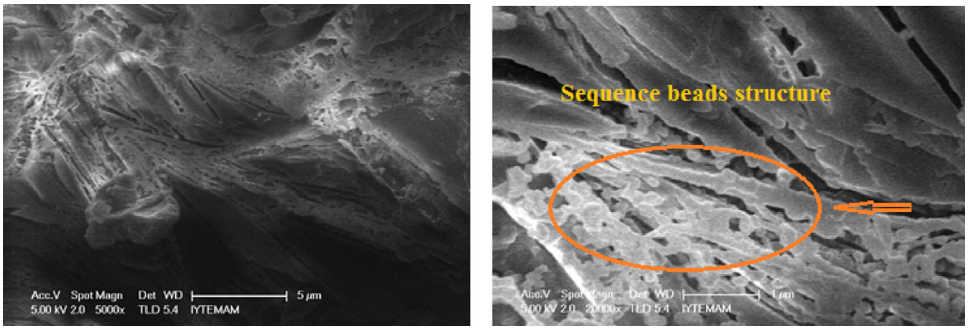

Fig. 5. SEM image of selected areas in PMIPTEG.

the activation energy. On the other hand, the Kim–Park method assumes that maximum degradation fraction, α_m is independent of the kinetic triplet: the activation energy, the pre-exponential factor and the decomposition mechanisms. The activation energy can be obtained by the slope of the plot of ln β versus $1/T_m$ by using Eq. (2).

$$\ln \beta = \ln A + \left(\frac{E}{R}\right) + \ln\left[1 - n + \frac{n}{0.944}\right] - 5.3305 - 1.0516\left(\frac{E}{RT_{max}}\right) \quad (2)$$

The activation energies related to the thermal decomposition stage of PMIPTEG obtained by using Kissinger and Kim–Park methods in N_2 were determined to be 100.1 and 104.4 kJ/mol, respectively.

The other methods used for calculating the kinetic parameter of PMIPTEG were those of Flynn–Wall–Ozawa, Kissinger–Akahira–Sunose, Tang and Friedman based on multiple heating rates. The conventional integral procedures such as FWO, KAS and Tang were proposed by assuming invariant activation energies and in the case of variable activation energies they might yield incorrect values (Criado, Sanchez-Jimenez, & Perez-Maqueda, 2008). In those cases, advanced integral isoconversional (Vyazovkin, 2001) or differential methods are preferred over integral isoconversional methods. Thus, in the present case, differential isoconversional methods (Friedman, Kissinger, Kim–Park), in addition to integral isoconversional methods (FWO, KAS and Tang) were used for solid state decomposition kinetic studies. The Flynn–Wall–Ozawa method is a conventional integral method and the activation energy of a solid state decomposition process without knowledge of the reaction order can determined by this method. In the technique the A, $f(\alpha)$ and E are independent of T while A and E are independent of α. So this method provides the following expression in logarithmic form for thermal decomposition kinetic studies based on the basic Arrhenius equation:

$$\log \beta = \log\left(\frac{AE}{R}\right) - \log g(\alpha) - 2.315 - 0.4567\left(\frac{E}{RT}\right) \quad (3)$$

According to the Eq. (3), constant mass loss lines were determined by measuring the temperature at a given mass percent for each rate. Fig. 6 presents the Arrhenius type plots of dynamic TG runs for mass ranging from $\alpha = 0.05$ to 0.95 in N_2. The apparent activation energy of PMIPTEG can be obtained from a plot of log β against $1000/T$ for a constant degree of conversion since the slope of such a line is given by $-0.456E/RT$.

The activation energies and correlation coefficient on the overall mass loss from 5 to 95 mass% determined with the FWO method in N_2 are summarized in Table 1 and the average value was found to be 103.2 kJ/mol over the range of α given. However, Table 1 indicated that the correlation coefficient with the Arrhenius type plots is acceptable and always superior to 0.98202.

On the other hand, the Tang and KAS methods are an integral isoconversional method similar to the FWO. The Tang method allows the activation energy to be determined by plotting ln (β/T^2) against

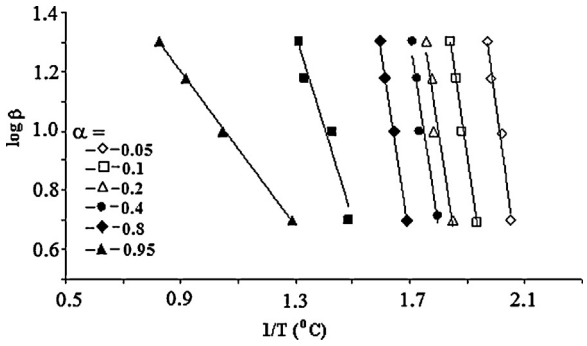

Fig. 6. FWO plots for the thermal decomposition of PMIPTEG at varying conversion in N_2.

$1/T$ for a fixed degree of conversion at the different heating rates β. The slope of such a line obtained by the KAS method is given by $-0.456E/RT$ (Eq. (4)). However, to calculate the values of the activation energy from plots of ln $(\beta/T^{1.894661})$ against $1/T$ over a wide range of conversions, Eq. (5) proposed by KAS can also be used. The activation energy E can be obtained from the slope $-1.001450E/R$ of the regression line. The kinetic procedures of the Tang and KAS methods are given below, respectively.

$$\ln\left(\frac{\beta}{T^{1.894661}}\right) = \ln\left(\frac{AE}{Rg(\alpha)}\right) + 3.635041 - 1.894661 \ln E - \frac{1.001450E}{RT} \quad (4)$$

$$\ln\left[\frac{\beta}{T^2}\right] = \ln\left[\frac{AR}{Eg(\alpha)}\right] - \frac{E}{RT} \quad (5)$$

In this study the equation $\alpha = 0.05$–0.95 was chosen to determine the E values of PMIPTEG. The activation energy of PMIPTEG obtained with the Tang and KAS methods were found to be 102.0 and 102.2 kJ/mol, respectively, over the range of $0.05 < \alpha < 0.95$. These results are more agreeable with the mean value of the activation energy obtained by the FWO method. The other differential isoconversional method, similar to the Kissinger and Kim–Park method used in this study was that of Friedman. This method, used for thermal decomposition kinetic studies, can be simplified as

$$\ln\left(\frac{d\alpha}{dt}\right) = \ln(A) + n \ \ln(1-n) - \frac{E}{RT} \quad (6)$$

Like the other methods, the technique assumes that the activation energy of a solid state decomposition process is independent of the reaction order. The activation energy related to thermal decomposition of PMIPTEG can therefore be calculated from the plot of $\ln[\beta d\alpha/dT]$ versus $1000/T$ with the data fitting into a straight line. The activation energies of thermal decomposition E of PMIPTEG in N_2 were determined to be 99.0 kJ/mol, over a wide range of conversions. This result is much smaller than the related values of PMIPTEG obtained with the other five methods in N_2. The activation energies calculated from the FWO, Tang, KAS and Friedman

Table 1
Activation energies and correlation coefficient obtained by KAS, FWO, Tang and Friedman methods for the thermal decomposition stage of PMIPTEG.

Thermal decomposition stage								
Conversion	E_{Tang}	r	E_{KAS}	r	E_{FWO}	r	E_{FR}	r
0.05	127.3	0.98721	128.1	0.98635	127.7	0.98323	123.6	0.98755
0.1	119.6	0.98734	117.3	0.984223	117.9	0.98411	116.2	0.98767
0.2	116.2	0.99273	115.4	0.99557	114.6	0.99424	112.9	0.99877
0.3	114.8	0.99465	114.2	0.99479	113.7.	0.99566	111.1	0.99222
0.4	113.2	0.99844	111.3	0.99860	112.8	0.99767	109.4	0.99311
0.5	115.8	0.99324	114.8	0.99455	114.6	0.99757	112.5	0.99233
0.6	114.2	0.99876	113.4	0.99722	114.0	0.99181	111.4	0.99566
0.7	115.1	0.99384	116.7	0.99284	115.4	0.99233	113.2	0.99744
0.8	114.3	0.99823	112.1	0.99547	110.3	0.99414	109.3	0.99222
0.9	58.61	0.99775	56.22	0.99742	57.52	0.99555	55.80	0.99311
0.95	26.72	0.98465	25.43	0.98809	23.48	0.98202	21.10	0.98644
$0.05 < \alpha < 0.95$	102.0		102.2		103.2		99.6	

E, activation energy (kJ/mol); r, correlation coefficient.

methods for the thermal decomposition stage of PMIPTEG are summarized in Table 1. In the equations above, α, $g(\alpha)$, β, T_m, E, A, and R correspond to the degree of reaction, integral function of conversion, heating rate, DTG peak temperature, activation energy (kJ/mol), pre-exponential factor (s^{-1}) and gas constant (8.314 J/mol K), respectively. Briefly, the activation energies (E values) of PMIPTEG calculated according to all kinetic procedures are very close to each other. Also, the correlation coefficients of the Arrhenius type plots of dynamic TG/DTG runs for activation energy during the decomposition stage of PMIPTEG given in Table 1 are considerably higher for masses ranging from $\alpha = 0.05$ to 0.095 in N_2. E values obtained by the Kissinger, Kim–Park, Tang, KAS, FWO and Friedman method are 100.1, 104.4, 102.0, 102.2, 103.2 and 99.6 kJ/mol, respectively for the thermal decomposition stage, over the conversion degree of $0.1 < \alpha < 0$. From the E-dependencies degree of conversion for the thermal decomposition stage of PMIPTEG, α in TG runs in N_2 presented in Table 1, it was shown that the thermal decomposition process of PMIPTEG had a similar behavior for all the methods in conversions ranging from $\alpha = 0.2$ to 0.8. This result indicates that the mechanism of the thermal decomposition stage of PMIPTEG does not change in the range of $0.1 < \alpha < 0.8$. The lowest activation energy value related to the initial decomposition of PMIPTEG obtained by using the Friedman method was determined to be approximately 123.6 kJ/mol, over the range of $0.05 < \alpha < 0.95$. In order to determine the most likely mechanism for the solid state decomposition process of PMIPTEG, in this study we chose master plots in which a comparison of the experimental master plots with theoretical ones corresponds to the mechanism of a solid state decomposition process. The integral function of conversion in the solid state non-isothermal decomposition reactions is expressed as

$$g(\alpha) = \left(\frac{A}{\beta}\right) \int_{T_0}^{T} \exp\left(\frac{-E}{RT}\right) dT = \left(\frac{AE}{\beta R}\right) p(u) \tag{7}$$

where $p(u) = \int_{\infty}^{u} (e^{-u}/u^2) du$ and $u = E/RT$.

According to Eq. (5), using a reference at point $\alpha = 0.5$ gives

$$g(\alpha) = \left(\frac{AE}{\beta R}\right) p(u_{0.5}) \tag{8}$$

where $u_{0.5} = E/RT$. When Eq. (7) is divided by Eq. (8), the following equation can be written

$$\frac{g(\alpha)}{g(0.5)} = \frac{p(\alpha)}{p(u_{0.5})} \tag{9}$$

According to the master plots method, by using an approximate formula of $P(u)$, $P(u) = \exp(-u)/[u(1.00198882u + 1.87391198)]$ (Wanjun, Yuwen, Hen, Zhiyong, & Cunxin, 2003), the experimental master plots of $P(u)/P(u_{0.5})$ against α can be drawn from experimental data of the thermal decomposition of PMIPTEG obtained under different heating rates. In this case, Eq. (9) shows that, for a given α, the experimental values of $g(\alpha)/g(\alpha_{0.5})$ along with ones obtained by using an appropriate kinetic model are equivalent to each other. Therefore, comparing the experimental master plots with theoretical ones we can determine the kinetic model related to the thermal decomposition stage of PMIPTEG. The comparisons of the experimental master plots with the theoretical ones showed that the kinetic processes of the thermal decomposition of PMIPTEG accorded with the D_1 master curve very well. Thus a diffusion type kinetic model for the thermal decomposition stage of PMIPTEG is suggested by master plot curves. In the literature, the D_1 model is also known as a one-dimensional mechanism. This kinetic model is quite rare in polymer degradation studies and it has been reported in the literature that the thermal degradation of polyethylene and some polyphenol derivates only follows a diffusion kinetic model (Sanchez-Jimenez, Perez-Maqueda, Perejon, & Criado, 2009; Sanchez-Jimenez, Perez-Maqueda, Perejon, & Criado, 2010).

Table 2
Activation energies and correlation coefficients obtained by plotting $\ln[\beta R/E] - \ln[P(u)]$ against $-\ln[\alpha^2]$.

β (K/mol)	$\ln A$ (s^{-1})	r
5	12.19	0.998821
10	12.28	0.99873
15	12.05	0.99766
20	12.22	0.99657
Mean	12.18	

By assuming the D_1 law for the thermal decomposition stage of PMIPTEG, the mathematical expression of the D_1 master-model curve, experimental data and the predetermined average reaction energy were subtracted in Eq. (9). Consequently, the following equation for the thermal decomposition stage was obtained:

$$\ln\left[\frac{\beta R}{E}\right] - \ln[P(u)] = \ln A - \ln[\alpha^2] \tag{10}$$

The pre-exponential factor related to the thermal decomposition stage was calculated from the intercepts of a group of straight lines obtained by plotting $\ln[\beta R/E] - \ln[P(u)]$ versus $-\ln[\alpha^2]$ under heating rates and found to be 12.18 s^{-1}. The activation energies and correlation coefficients obtained from the plot of $\ln[\beta R/E] - \ln[P(u)]$ against $-\ln[\alpha^2]$ is shown in Table 2.

4. Conclusion

A new carbohydrate-based polymer, PMIPTEG was synthesized by a conventional free radical polymerization reaction using AIBN as an initiator in 1,4-dioxane. The resulting polymer was relatively soluble in organic solvents. PMIPTEG was characterized using various spectral and thermal techniques. M_n, M_w and PDI values of PMIPTEG were determined to be 9300 g/mol, 13,400 g/mol and 1.44, respectively. SEM photographs showed that PMIPTEG was composed of the linear polymer chains with thin channels. The average values of activation energy of the thermal decomposition of PMIPTEG were also investigated by thermogravimetric technique at the heating rates of 5, 10, 15 and 20 °C/min in an N_2 atmosphere. The activation energies related to the thermal decomposition of PMIPTEG according to the Kissinger, Kim–Park, Tang, KAS, FWO and Friedman methods were determined to be 100.1, 104.4, 102.0, 102.2, 103.2 and 99.6 kJ/mol, respectively, in the conversion range studied. The results obtained with the master plot curves indicated that the decomposition mechanism of PMIPTEG in N_2 went to the D_n mechanism (deceleration type). This is the first such report for a carbohydrate-based polymer. The logarithmic value of the pre-exponential factor related to the decomposition mechanism of the resulting polymer was found to be 12.18 s^{-1}.

References

Akahira, T., & Sunose, T. (1971). *Research Report of Chiba Institute Technology*, *16*, 22.
Anıl, H., Yüceer, L., & Yüceer, T. (1983). *Carbohydate Research*, *123*, 153–156.
Budrugeac, P., & Segal, E. (2008). *Polymer Degradation and Stability*, *93*(6), 1073–1080.
Carneiro, M. J., Fernandes, A. C., Figueiredo, M., Fortes, A. G., & Freitas, A. M. (2001). *Carbohydrate Polymers*, *45*, 135–138.
Criado, J. M., Sanchez-Jimenez, P. E., & Perez-Maqueda, L. A. (2008). *Journal of Thermal Analysis and Calorimetry*, *92*, 199–203.
Dilek, D., Doğan, F., Bilici, A., & Kaya, İ. (2011). *Thermochimica Acta*, *518*(1–2), 72–81.
Doğan, F., Akat, H., Balcan, M., Kaya, İ., & Yürekli, M. (2008). *Journal of Applied Polymer Science*, *108*, 2328–2336.
Doğan, F., Şirin, K., Kaya, İ., & Balcan, M. (2010). *Polymers for Advanced Technologies*, *21*, 512–519.
Doğan, F., Kaya, İ., & Bilici, A. (2011). *Synthetic Metals*, *161*(1–2), 79–86.
Flynn, J., & Wall, L. A. (1966). *Journal of Polymer Science Part B: Polymer Letter*, *4*, 323–328.
Forsen, S., Lindberg, B., & Silvander, B. G. (1965). *Acta Chemica Scandinavica*, *19*, 359–369.
Friedman, H. L. (1965). *Journal of Polymer Science Part C: Polymer Symposia*, *6*, 183–195.
Kaya, İ., Doğan, F., & Bilici, A. (2009). *Polymer International*, *58*, 570–578.
Kim, S. D., & Park, J. K. (1995). *Thermochemica Acta*, *264*, 137–156.
Kimura, S., & Imoto, M. (1961). *Makromolecular Chemistry*, *50*, 155–160.
Kissinger, H. F. (1957). *Analytical Chemistry*, *29*, 1702–1706.
Kök, G., & Salman, Y. (2012). *Journal of Carbohydrate Chemistry*, *31*(1), 1–9.
Lowe, A. B., & Wang, R. (2007). *Polymer*, *48*, 2221–2230.
Metz, C. J. S., Ise, T., & Haberle, D. A. (1996). *European Journal of Physiology*, *432*, 944–947.
Ohno, K., Tsujii, Y., & Fukuda, T. (1998). *Journal of Polymer Science, Polymer Chemistry*, *36*(14), 2473–2481.
Ozawa, T. (1965). *Bulletin of the Chemical Society of Japan*, *38*, 1881–1886.
Pachence, J. M., & Kohn, J. (1997). In R. Lanza, R. Langer, & W. Chick (Eds.), *Principles of tissue engineering* (pp. 273–285). Academic Press/R.G. Landes Company.
Patil, D. R., Dordick, J. S., & Rethwisch, D. G. (1991). *Macromolecules*, *24*, 3462–3463.
Salagean, I. R., Pascariu, M. C., Bandur, G., & Rusnac, L. M. (2009). *Chemical Bulletin "POLITEHNICA" University (Timisoara)*, *54*(68), 2.
Salman, G. Y., Makinabakan, O., & Yüceer, L. (1994). *Tetrahedron Letters*, *35*, 9233–9236.
Salman, G. Y., Kök, G., & Yüceer, L. (2004). *Carbohydrate Research*, *339*, 1739–1745.
Sanchez-Jimenez, P. E., Perez-Maqueda, L. A., Perejon, A., & Criado, J. M. (2009). *Polymer Degradation Stability*, *94*, 2079–2085.
Sanchez-Jimenez, P. E., Perez-Maqueda, L. A., Perejon, A., & Criado, J. M. (2010). *Journal of Physical Chemistry A*, *114*, 7868–7876.
Şirin, K., Doğan, F., Balcan, M., & Kaya, İ. (2009). *Journal of Macromolecular Science, Part A. Pure and Applied Chemistry*, *46*, 949–958.
Tang, W., Liu, Y., Yang, X., & Wang, C. (2004). *Industrial & Engineering Chemistry Research*, *43*(9), 2054–2059.
Varma, A. J., Kennedy, J. F., & Galgali, P. (2004). *Carbohydrate Polymers*, *56*, 429–445.
Vyazovkin, S. (2001). *Journal of Computational Chemistry*, *22*, 178–183.
Wanjun, T., Yuwen, L., Hen, Z., Zhiyong, W., & Cunxin, W. (2003). *Journal of Thermal Analysis and Calorimetry*, *74*(1), 309–315.
Wulff, G., Schmid, J., & Venhoff, T. (1996). *Macromolecular Chemistry and Physics*, *191*, 259–274.
Yenil, N., Ay, E., Ay, K., Oskay, M., & Maddaluno, J. (2010). *Carbohydrate Research*, *345*, 1617–1621.